

# NOVEL NON-INVASIVE MICRO-CT CONTRAST AGENT FOR QUANTITATIVE VIRTUAL 3D HISTOLOGY OF MINERALIZED AND SOFT SKELETAL TISSUES

G. Kerckhofs<sup>1,2</sup>, S. Stegen<sup>2,3</sup>, N. Van Gastel<sup>2,3</sup>, A. Sap<sup>4</sup>, G. Falgayrac<sup>5</sup>, G. Penel<sup>5</sup>, M. Durand<sup>2,6</sup>, FP.  
Luyten<sup>1,2</sup>, L. Geris<sup>2,7,8</sup>, K. Vandamme<sup>2,9</sup>, T. Parac-Vogt<sup>4+</sup>, G. Carmeliet<sup>2,3+</sup>

<sup>1</sup>Skeletal Biology and Engineering Research Center, Dept. Development and Regeneration, KU Leuven, Belgium

<sup>2</sup>Prometheus, Division of Skeletal Tissue Engineering, KU Leuven, Belgium

<sup>3</sup>Clinical and Experimental Endocrinology, Dept. of Clinical and Experimental Medicine, KU Leuven, Belgium

<sup>4</sup>Molecular Design and Synthesis, Dept. of Chemistry, KU Leuven, Belgium

<sup>5</sup>UDSL, EA 2603, PMOI, Université de Lille, Nord de France, France

<sup>6</sup>UMR CNRS 7052, Biomécanique et Biomatériaux Ostéo-Articulaires, Faculté de Médecine Lariboisière Paris, France

<sup>7</sup>Biomechanics Research Unit, Université de Liege, Belgium

<sup>8</sup>Biomechanics Section, Dept. of Mechanical Engineering, KU Leuven, Belgium

<sup>9</sup>Biomaterials – BIOMAT, Dept. of Oral Health Sciences, KU Leuven, Belgium

<sup>+</sup>*These authors have contributed equally and share last authorship.*

## ABSTRACT

Organs and biological tissues have a complex and heterogeneous 3D structure, and thus 2D measurements like histomorphometry only partially reveal the full 3D structure. As a solution, we propose contrast-enhanced microfocus computed tomography (CE-CT) for quantitative virtual 3D histology of multiple tissues in a single dataset. As most existing contrast agents are invasive, toxic and/or non-specific, we show the non-invasive character of a novel contrast agent that allows to simultaneously visualize the bone and bone marrow compartment, including the vascularization and adiposity, in murine long bones. Moreover, we have quantified the 3D structure of these different tissues in different mouse models (i.e. ageing and type 2 diabetes), showing the added value of CE-CT compared to standard histomorphometry. The additional information that CE-CT is providing compared to standard histomorphometry, with a spatial dimension, could bring novel insights in the biological processes during tissue development, remodeling and regeneration.

**Index Terms** — Contrast enhanced computed tomography (CE-CT), virtual 3D histology, skeletal tissues, 3D visualization & quantification

## 1. INTRODUCTION

Organs and biological tissues have a complex heterogeneous 3D structure. Thus, measurements of these tissues made in 2D only partially reveal the full 3D structure and interconnections between different tissues. Innovations in imaging techniques are fundamental to fully understand the complex 3D tissue structures. Currently, the standard technique for evaluating organs and biological tissues is histological sectioning. It has a high discriminative power, both on tissue and cellular level. However, it shows limited potential for quantifying 3D properties of the tissues as it is destructive and costly in terms of time and resources. Most importantly, in standard settings, it only allows assessment of tissue distribution in 2D, with loss of information due to a restricted sectioning orientation and with limited depth resolution.

X-ray microfocus computed tomography (micro-CT) has been frequently applied as 3D quantitative imaging technique to assess mineralized skeletal tissues [1-3]. However, soft tissue contrast is inherently poor. A recent shift in microCT imaging focuses on the use of X-ray opaque contrast agents for visualizing soft tissues, such as cartilage [4-8], blood vessels [9-11] and connective tissues [1, 12]. For cartilage, containing negatively charged glycosaminoglycans, specific ionic and anionic contrast agents have been developed [4-8].

For other soft tissues, however, there are currently no tissue-specific X-ray opaque contrast agents. Using trial-and-error, several groups have assessed different chemicals to stain these tissues with varying degrees of success, but without in-depth validation or sufficient knowledge of the tissue-specific binding mechanisms [13, 14]. Additionally, most of those contrast agents are destructive [15] or toxic, preventing subsequent (immuno)histological assessment.

In this study, we present a novel in-house developed contrast agent for contrast-enhanced microCT (CE-CT) of the bone and bone marrow compartment of murine long bones. This technique allows simultaneous 3D multi-tissue imaging, i.e. in a single image set, of the bone and the bone marrow vascularization and adiposity. We will show the binding mechanisms of the novel contrast agent, along with its non-invasive character and its potential to be used as for virtual quantitative 3D histology of skeletal soft tissues.

## 2. METHODS & RESULTS

The novel in-house developed contrast agent is a metal-substituted polyoxotungstate, and is further referred to as Hf-POT (Hf-substituted). In this study, we compared Hf-POT with phosphotungstic acid (PTA), a well-known existing CE-CT contrast agent [12, 14, 15]. Using Raman spectroscopy, we determined that Hf-POT binds electrostatically to the biological tissues, and that it does not alter the chemical composition of the tissues, as opposed to PTA. This is a first indication of the non-invasive character of Hf-POT.

To further elaborate on this non-invasive character, we investigated the potential to perform histological and immunological staining after CE-CT imaging with Hf-POT. Therefore, we first stained tibias of 4 weeks old mice with both PTA and Hf-POT (both at a concentration of 3.5% in PBS solution), and scanned these using CE-CT (Fig. 1A and 1C). Briefly, after harvesting and fixation in

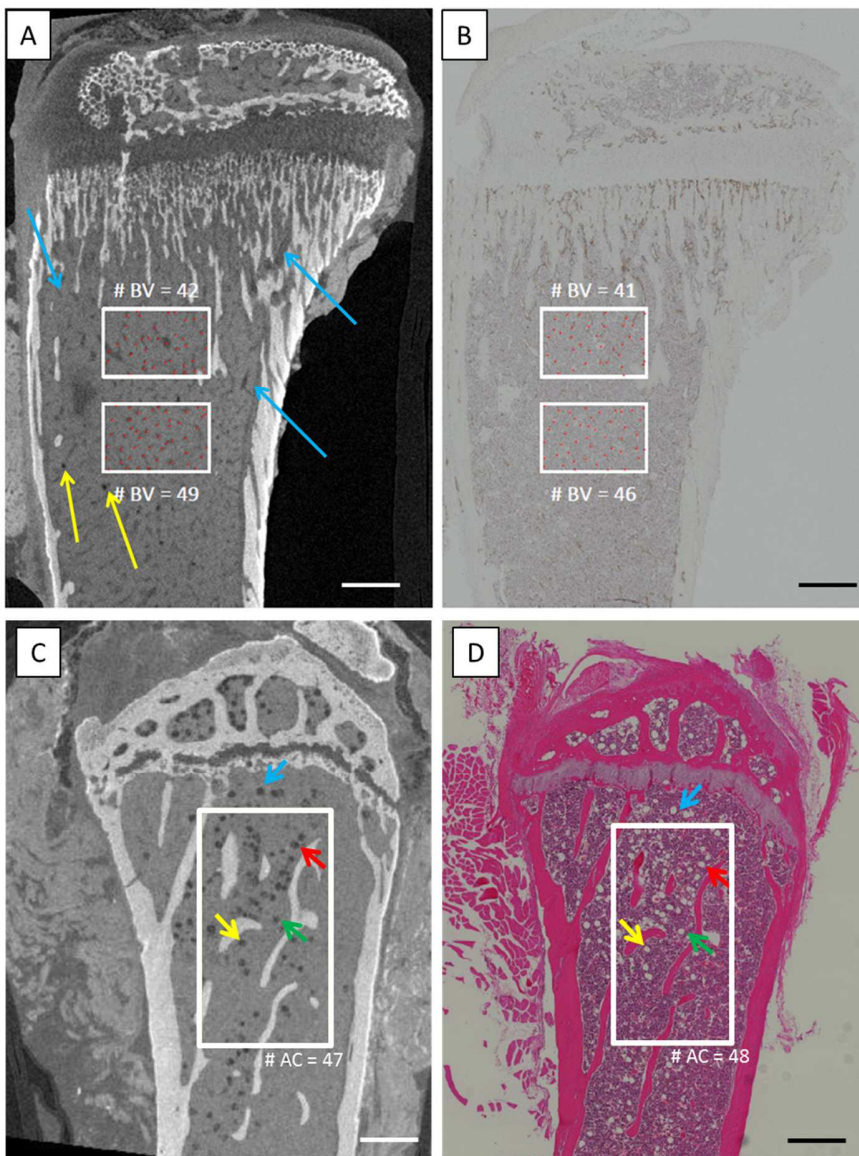


Figure 1: (A) Typical coronal CE-CT image of a mouse tibia, stained using Hf-POT. Blue arrows indicate blood vessels; yellow arrows indicate adipocytes.

(B) The corresponding immunohistological section using CD31 staining. A brown color indicates CD31 positive blood vessels. The red dots in both images, within the regions of interest, indicate the blood vessels assigned by manual counting.

(C) Typical coronal CE-CT image of a mouse tibia, stained using Hf-POT. (D) The corresponding H&E section. A pink color indicates bone and the white spheres (not containing red blood cells) are adipocytes. The colored arrows indicate similar corresponding adipocytes between CE-CT and the H&E stained section. Scale bars = 250  $\mu\text{m}$ .

paraformaldehyde (2%, overnight), the samples were scanned on a NanoTom M [GE] at a 2  $\mu\text{m}$  voxel size, 60 kV and an exposure time of 500ms. A 0.3mm Al filter was used and 2400 images were acquired, resulting in a scan time of 20 minutes (i.e. fast scan mode). After scanning, the samples were processed both for CD31 immunostaining for blood vessel visualization and for H&E staining for the visualization of adipocytes. We included control samples that were not stained using the contrast agents, and performed blind scoring. PTA staining did not allow CD31staining and resulted in faint H&E staining, while the novel contrast agent

showed excellent CD31 and H&E tracing (Fig. 1B and 1D). Hf-POT stained samples did not show any difference with control samples that were not scanned nor stained with the contrast agents prior to H&E staining or CD31 immunostaining. Moreover, a direct comparison between histology (CD31 and H&E staining) and CE-CT indicated that the novel contrast agent allowed to visualize the blood vessels and the adipocytes in the bone marrow, and that both CE-CT and histology can be used in a similar way for scoring these tissues.

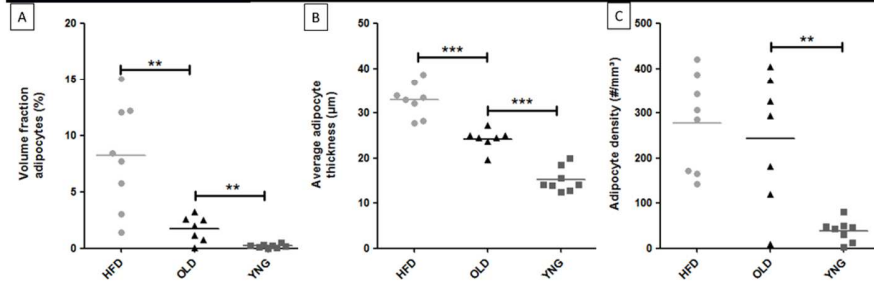
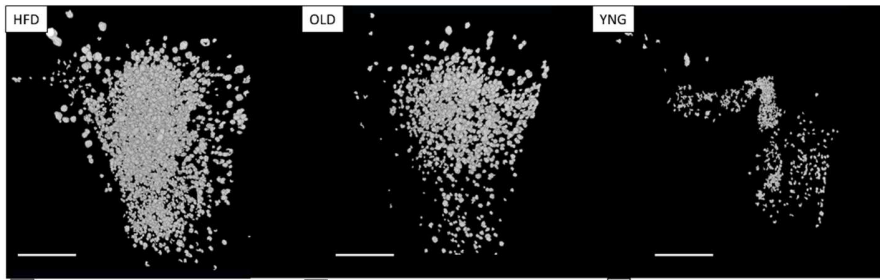


Figure 2. Representative 3D renderings of the bone marrow adipocytes of a HFD, OLD and YNG mouse generated using CE-CT. Scale bar is 500  $\mu\text{m}$ . Based on image analysis of the CE-CT images, (A) the volume fraction, (B) the average thickness and (C) the density of the adipocytes in the medullar space. \*  $p < 0.05$ , \*\*  $p < 0.01$ , \*\*\*  $p > 0.001$ .

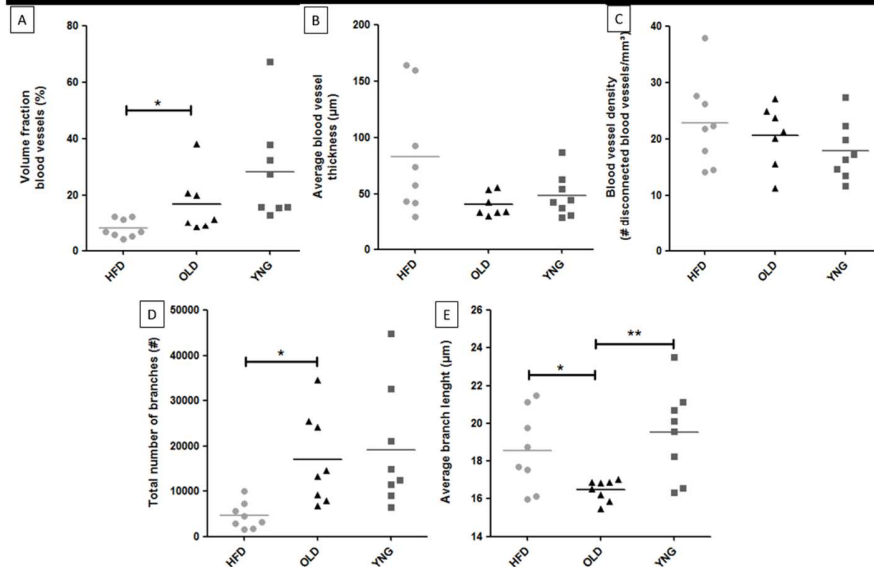
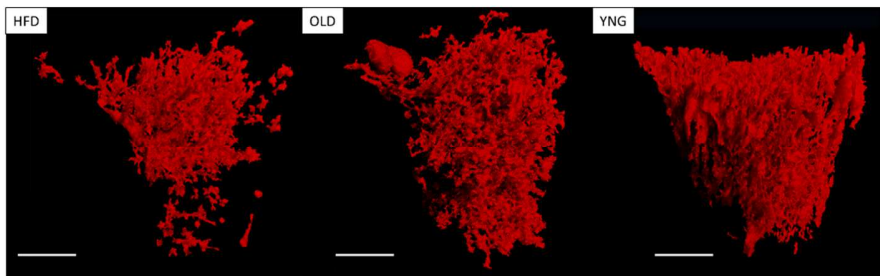


Figure 3. Representative 3D renderings of the bone marrow vascular network of a HFD, OLD and YNG mouse generated using CE-CT. Scale bar is 500  $\mu\text{m}$ . Based on image analysis of the CE-CT images, (A) the volume fraction, (B) the average thickness and (C) the density of the blood vessels in the medullar space, (D) the total number of branches and (E) the average branch length of the vascular skeleton. \*  $p < 0.05$ , \*\*  $p < 0.01$ , \*\*\*  $p > 0.001$ .

To show the added value of the novel contrast agent for quantitative virtual 3D histology using CE-CT, we scanned tibias of old (30 weeks - OLD), young (7 weeks - YNG) and Type 2 diabetic (30 weeks – high fat diet-induced obese model, HFD) mice and visualized the bone, and the blood vessel and adipocyte distribution in the bone marrow. Hf-POT was able to pick up differences between the three groups. Ageing induced a significant increase in the bone marrow adiposity (Fig. 2A and 2C) and adipocyte thickness (Fig. 2B). Although it did not show a significant change in the blood vessel content (Fig. 3A-C), it did show a significant decrease in the average branch length of the blood vessel network (Fig. 3E). Obesity-induced Type 2 diabetes even increased the bone marrow adiposity (Fig. 2A and 2C) and adipocyte thickness (Fig. 2B) in a significant manner. Moreover, it resulted in a significant decrease in the blood vessel content (Fig 3A) and number of branches of the blood vessel network (Fig. 3D), and in a significant increase in the average branch length of the blood vessel network (Fig. 3E).

Finally, as the CE-CT images are multi-tissue images, the three skeletal tissues of interest, i.e. bone, blood vessels and adipocytes, could be simultaneously visualized in 3D, as shown in Figure 4. This simultaneous visualization allowed to investigate and quantify (ongoing work) the proximity of the blood vessels to the bone, or of the adipocytes to the blood vessels, which provides additional information compared to standard 2D histomorphometry.

### 3. CONCLUSION

CE-CT is a multi-tissue 3D imaging technique that can be used for quantitative virtual 3D histology. Using a novel contrast agent, Hf-POT, it can reveal simultaneously the 3D structure of different skeletal tissues (i.e. bone, blood vessels and adipocytes) and their spatial distribution in murine long bones. Since it can provide additional information to standard histomorphometry, with a spatiotemporal dimension, CE-CT could provide novel insights in the dynamic biological processes during tissue development, remodeling and regeneration.

### 4. ACKNOWLEDGEMENTS

This study was financed by the Research Foundation - Flanders (FWO/12R4315N) and the European Research Council under the European Union's Seventh Framework Program (FP7/2007-2013)/ERC grant agreement n°279100. This work is part of Prometheus, the Leuven Research & Development Division of Skeletal Tissue Engineering of the KU Leuven: [www.kuleuven.be/prometheus](http://www.kuleuven.be/prometheus). The CE-nanoCT images have been generated on the X-ray computed tomography facilities of the Department of Materials Engineering of the KU Leuven, financed by the Hercules Foundation (project AKUL 09/001: Micro- and nanoCT for the hierarchical analysis of materials).

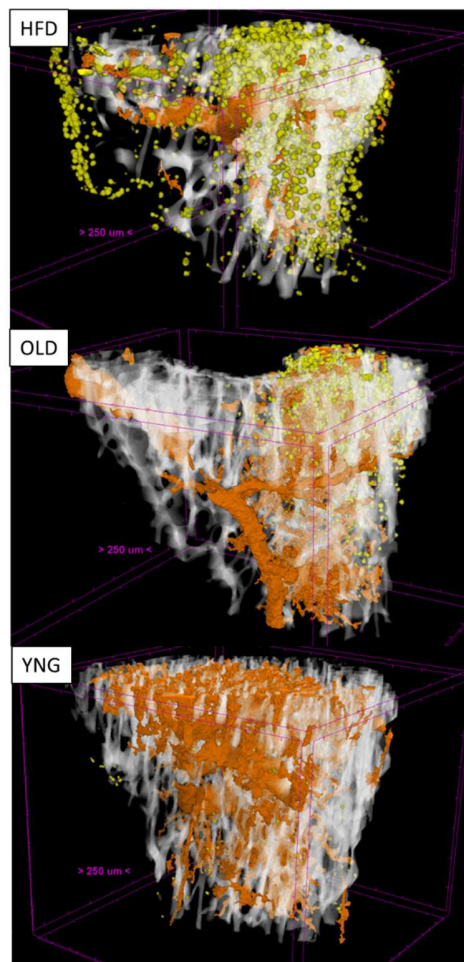


Figure 4. Representative 3D renderings of the bone (white), the bone marrow vascular network (orange) and the bone marrow adiposity (yellow) of a HFD, OLD and YNG mouse. 3D scale bars are included in the figure.

### 5. REFERENCES

- [1] Wong MD et al. *Development* 139(17), 3248 (2012).
- [2] Gregg CL and JT Butcher *Differentiation* 84(1), 149 (2012).
- [3] Oest ME et al. *Birth Defects Res B Dev Reprod Toxicol* 83(6), 582 (2008).
- [4] Kerckhofs G et al. *Cartilage* 5(1), 55 (2014).
- [5] Kerckhofs G et al. *Eur Cell Mater* 25(179) (2013).
- [6] Xie L et al. *Osteoarthritis and Cartilage* 18(1), 65 (2010).
- [7] Lakin BA et al. *Osteoarthritis Cartilage* 21(1), 60 (2013).
- [8] Joshi NS et al. *J Am Chem Soc* 131(37), 13234 (2009).
- [9] Fei J et al. *Anat Rec (Hoboken)* 293(2), 215 (2010).
- [10] Granton PV et al. *Med Phys* 35(11), 5030 (2008).
- [11] Lusic H and MW Grinstaff *Chem Rev* 113(3), 1641 (2013).
- [12] Metscher BD *Dev Dyn* 238(3), 632 (2009).
- [13] Metscher BD *BMC Physiol* 9(11) (2009).
- [14] Pauwels E et al. *J Microsc* 250(1), 21 (2013).
- [15] Buytaert J et al. *Microsc Microanal* 20(4), 1208 (2014).